Stoch Environ Res Risk Assess (2012) 26:357–373
DOI 10.1007/s00477-011-0481-9

ORIGINAL PAPER

The dynamic of vegetation coverage and its response to climate factors in Inner Mongolia, China

Yang Yang · Jianhua Xu · Yulian Hong · Guanghui Lv

Published online: 24 April 2011

Abstract Normalized Difference Vegetation Index (NDVI) is widely recognized as a good indicator of vegetation productivity. Diagnosing the NDVI trend and understanding climatic factors influences on NDVI can predict the productivity changes under different climatic scenarios. This paper examined NDVI dynamic and its response to climate factors during a 10 year period (1998–2008) in Inner Mongolia. The main findings are as follows: (1) The NDVI multi-scale characters can be revealed well by wavelet transform, and the average NDVI and the NDVI amplitude show a gradually decreased trend from northeast to southwest in Inner Mongolia during the past 10 years, furthermore, this trend is consistent with the heat and water distribution caused by latitude difference in north–south direction and Asia monsoon effect in east–west direction. (2) The relation between NDVI and temperature is the most close, followed by precipitation, sunshine hours and relative humidity. Different vegetation cover types show different strengths in correlation between NDVI and climate variables with the correlation values decreasing from forest, meadow steppe to desert steppe in whole. (3) The precipitation and temperature have the same change cycle, both nearly 290 days in the 20 selected stations. The NDVI has the same change cycle with the precipitation and temperature or either 10 days earlier or later than precipitation and temperature, which supports the significant correlation between NDVI and its climatic factors from a new perspective. The nearly 290 days change cycle implies that the vegetation growth cycle is nearly 10 months and there are no obvious differences change cycles in different vegetations. (4) Vegetation dynamic is significantly correlated to the temperature and precipitation at the time scale of 10, 20, 40, 80, 160, and 320-day, respectively, and the S3 scale (i.e., the time scale of 80-day), nearly 3 months (one season), is most significant and suitable for evaluating the vegetation dynamic to climatic factors.

Keywords Vegetation coverage · NDVI · Climate factor · Correlation · Wavelet transform · Inner Mongolia of China

1 Introduction

Evidence shows that there is a strong relationship between terrestrial ecosystem and climate variability (Cao and Woodward 1998; Pielke et al. 1998) and it has been reported that changes in terrestrial vegetation can modify local, regional, and global climate at a diurnal, seasonal, and long-term scale (Kaufmann et al. 2003). So studying the trend of vegetation dynamic and its response to climate variables can give us insight into the mechanism of ecosystem response to climate.

Until recently, a critical limitation to study temporal vegetation dynamics and its relationship with climate variables is lack of long-term data (Knapp and Smith 2001; Jobbágy et al. 2002). Fortunately, this limitation may be mitigated by the availability of remote sensing data, such as the SPOT sensor can provide the time series of satellite

Y. Yang · J. Xu (✉) · Y. Hong
The Research Center for East-West Cooperation in China, The Key Lab of GIScience of the Education Ministry PRC, East China Normal University, Shanghai 200062, China
e-mail: jhxuecnu@gmail.com; jhxu@geo.ecnu.edu.cn

G. Lv
The Key Lab of Oasis Ecology of the Education Ministry PRC, Xinjiang University, Urumqi 830046, Xinjiang, China

images to study vegetation dynamics. Among the surface parameters extracted from the remote sensing data, the vegetation production index, especially the Normalized Difference Vegetation Index (NDVI), which is calculated as the formula $NDVI = (NIR - RED)/(NIR + RED)$, where NIR and RED are the reflectance in the near-infrared and red electromagnetic spectrums of objects on the earth surface, respectively, (Eidenshink and Faundeen 1994), is mostly used. NDVI is a measurement for absorbed photosynthetic active radiation because the internal mesophyll structure of healthy green leaves strongly reflects NIR radiation, and leaf chlorophylls and other pigments absorb a large proportion of the red VIS radiation (Wang et al. 2003), and it has been widely used by researchers to estimate green biomass (Prince 1991; Tucker et al. 1985), leaf area index (Asrar et al. 1984), vegetation greenness (Diodato and Bellocchi 2008) and patterns of productivity (Goward and Dye 1987). Environmental factors, particularly the controlling climate factors such as precipitation and temperature, that affecting the vegetation growth also have influence on NDVI values (Nemani et al. 2003). Because stronger relations exist between climate factors and NDVI, as well as NDVI can reflect the vegetation growth, we can adopt those factors to estimate the vegetation activity.

During the past decades, various methods are used to detect vegetation dynamics from multi-temporal data. Among them we can find (i) statistical approaches such as principal component analysis (Hirosawa et al. 1996; Hall-Beyer 2003) and curve fitting (Jönsson and Eklundh 2004), (ii) time series analysis such as distribute lag model (Udelhoven et al. 2009), (iii) spectral-frequency techniques such as Fourier analysis (Azzali and Menenti 2000; Stockli and Vidale 2004) and, most recently, wavelet decomposition, which has been used to characterize crop phenology (Sakamoto et al. 2005) as well as to determine changes in the expansion and intensification of crops (Galford et al. 2008). NDVI time series and the climate factors time series data are usually non-stationary, i.e., they present different components with different frequencies, such as seasonal variations, long-term and short-term fluctuations, which may not be limited only to the mean of the series but also affect its overall variance structure (Martínez and Gilabert 2009). And these series show patterns like seasonality, trends and localized abrupt changes or discontinuities resulting from disturbance events (de Beurs and Henebry 2005). Although the limited spatial resolution of the available satellite-based time series can restrict the range of detected changes (Coppin et al. 2004), their high temporal resolution offers opportunity to define time profiles (Borak et al. 2000) and characterize the vegetation dynamics on the basis of different temporal scales. Therefore, based on time series analysis, the remote sensing techniques allow for characterizing the inter-annual and intra-annual variations of the vegetation canopy with a functional representation which is continuous and stable between years (Bradley et al. 2007) and at the same time, accounting for non-stationary processes. Wavelet transform is a new method to study the temporal pattern of NDVI and the climate variables, based on the ability of observer on various time cycles.

On the other hand, many studies have used NDVI to monitor vegetation response to climatic fluctuations in regional zone such as Africa (Malo and Nicholson 1990; Davenport and Nicholson 1993; Nicholson and Farrar 1994; Chamaille-Jammes et al. 2006), China (Zhong et al. 2010), US (Wang et al. 2003), Northern Patagonia (Fabricante et al. 2009) and at a global scale (Schultz and Halpert 1993). We can get a clue from these studies that temporal variations of NDVI are closely linked with climate factors. However, most other studies have related NDVI curves with precipitation and temperature curves during the growing season to find the best correlations (Wang et al. 2003). They could not take the overall trend of vegetation growth into consideration. On the other hand, other climate factors such as sunshine hours and relatively humility were not taken into consideration and the length of growing season was through the observation or empirical knowledge (Zeng and Yang 2008), whereas few studies have computed the vegetation growth cycle from the NDVI time series.

In all, our understanding of the mechanism and extent of the weather influence on NDVI is far from complete (Wang et al. 2003). The interaction between temperature, radiation, and water impose complex and various limitations on vegetation activity in different parts of the world (Churkina and Running 1998), and the development of effective methodologies for the analysis on multi-temporal data, are the most important and challenging issues for the remote sensing community (Bruzzone et al. 2003).

Based on the two points above, this paper employed a new comprehensive method to examine temporal patterns in detail about the vegetation dynamic and its response to climatic factors. Firstly, wavelet transform, a multi-resolution method, was employed to analyze NDVI dynamic based on remote sensing images over times at the inter- and intra-annual scales, giving us a whole images about the NDVI dynamic in the Inner Mongolia. Secondly, wavelet variance analysis was used to reveal the periodicity trend in the NDVI and climatic variables, trying to analyze their relationship from a new perspective. Thirdly, in order to investigate the impact of climate factors on NDVI with most suitable time scale, NDVI and the climatic variables on the selected meteorological stations were analyzed over six time scales based on correlation and regression method.

2 Materials and methods

2.1 Study area

The study area (Fig. 1) we selected is the Inner Mongolia Autonomous Region (IM), which is the third largest province of China (1.18 million square km) and it lies between latitudes 37°24′–53°23′N and longitudes 97°12′–126°04′E, with a mean elevation of 1014 m. As the history research, semi-arid climate is the major climate type in IM, where also has arid climate in the southwestern and semi-humid climate in the northern. In the east, there are boundless primitive forests in the Great Khingan Mountain Range, and in the west, there is a large area of desert centering on the Ordos Plateau. The extended areas from the plateaus are plains mainly formed by the reaches of the Yellow River and the Liao River, known as the Hetao area and Nen area. In the region, the area of grassland is up to 880,000 km^2, accounting for 21.7% of the total nation and taking as the leader of five largest grasslands in China. The climate is characterized by a decrease in precipitation and an increase in temperature from northeast to southwest. The precipitation in the northeast of IM exceeds 400 mm to support deciduous forest (0.23 million square km, 19.7% of the region) and irrigate agriculture. The north central region of IM, bordering the Gobi Desert, is dominated by the semiarid steppe with annual rainfall less than 100 mm. At middle longitudes of IM, the zonal vegetation types are dominated by meadow steppes, typical steppes and desert steppes (Wang et al. 2009). Meadow steppes are mainly distributed at the eastern end of the Inner Mongolia Plateau, with annual precipitation of 350–550 mm, 1800–2500°C cumulative active temperature above 10°C, and a dryness degree of 0.7–1.2. The topography is generally flat, and typical steppes are mainly distributed in the Xilingol League, which has a semi-arid climate with cold winters, warm summers, abundant windblown sand and sunlight. Annual precipitation is 150–400 mm, which is suitable for low-temperature herbaceous xerophilous vegetation. Moreover, desert steppes are found primarily in the western parts of the Erleahot and Ordos regions, where annual precipitation is 150–280 mm and annual mean temperature ranges from 2.6 to 4.7°C.

2.2 Date description

2.2.1 *Climate data*

The climate data used in this study was from 20 selected meteorological stations (Table 1) in IM, providing by the China Meteorological Data Sharing Service System (http://cdc.cma.gov.cn). The climate data included ten-days mean temperature (T, 0.1°C), ten-days mean precipitation (P, 0.1 mm), ten-days average relative humidity (H, 1%) and ten-days sunshine hours (S, 0.1 h). These stations were selected to represent the four major vegetation types in the IM and were evenly distributed across typical vegetation area, with 2, 4, 9 and 5 stations in forest, meadow steppe, typical steppe and desert steppe, respectively. These stations, with different altitudes, covered a large portion of the IM from northeast to southwest. The time series of the data we used were from 1998 to 2008. The vegetation map of

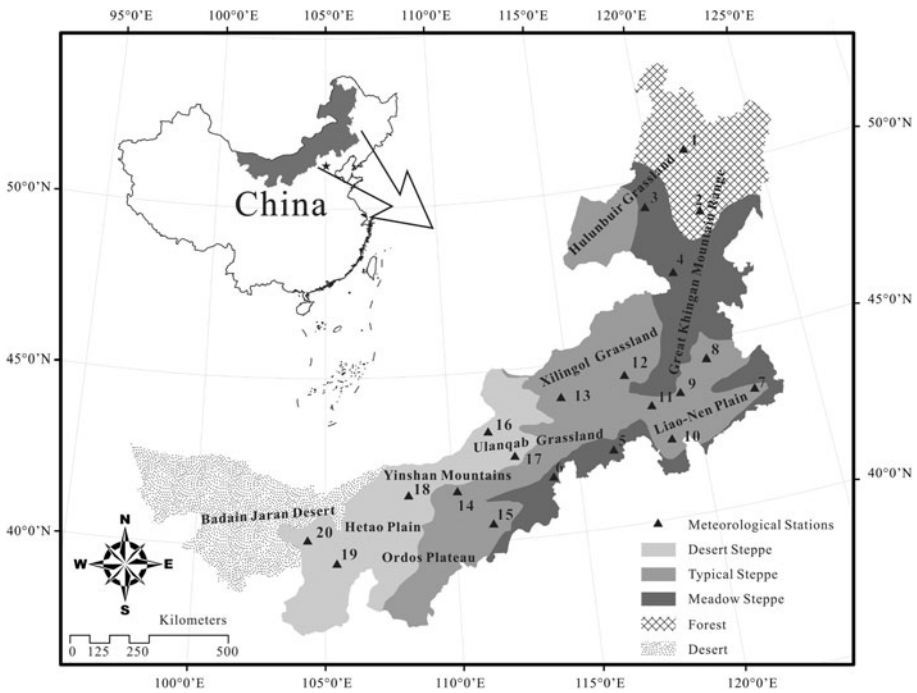

Fig. 1 A general map of selected metrological stations and vegetation in Inner Mongolia

Table 1 Selected meteorological stations with their corresponding vegetation types

No.	Station	Longitude (°)	Latitude (°)	Altitude (m)	Vegetation types
1	Tulihe	121.41	50.29	732.60	Forest
2	Bugt	121.55	48.46	739.7	Forest
3	Hailar	119.45	49.13	610.20	Meadow steppe
4	Arxan	119.57	47.10	1027.40	Meadow steppe
5	Duolun	116.28	42.11	1245.40	Meadow steppe
6	Huade	114.00	41.54	1482.70	Meadow steppe
7	Tongliao	122.16	43.36	178.50	Typical steppe
8	Jarud Banner	120.54	44.34	265.00	Typical steppe
9	Bairin Left Banner	119.24	43.59	484.4	Typical steppe
10	Chifeng	118.56	42.16	568.00	Typical steppe
11	Linxi	118.04	43.36	799.00	Typical steppe
12	West Ujimqin Banner	117.36	44.35	1000.60	Typical steppe
13	Abag Banner	114.57	44.01	1126.10	Typical steppe
14	Darhan United Banner	110.26	41.42	1376.60	Typical steppe
15	Hohhot	111.41	40.49	1063.00	Typical steppe
16	Erenhot	111.58	43.39	989.50	Desert steppe
17	Zhurihe	112.54	42.24	1150.80	Desert steppe
18	Urad Middle Banner	108.31	41.34	1288.00	Desert steppe
19	Jartai	105.45	39.47	1031.80	Desert steppe
20	Bayan Mod	104.48	40.1	1323.90	Desert steppe

IM was digitalized from China Vegetation Map with scale of 1:1000000.

2.2.2 *NDVI data*

The time series from 1998 to 2008 of the NDVI data were obtained from SPOT VEGETATION synthesis products (VGT-S). The pixels for the syntheses are based on the selection of the maximum NDVI value during the ten consecutive days, aiming to ensure coverage of all landmasses worldwide with a minimum effect of cloud cover. The pixel brightness count is the ground area's reflectance (corrected for atmospheric effects) and pixels in the sea area are set to 0. In order to allow daily monitoring of terrestrial vegetation cover through remote sensing from regional to global scales, VEGETATION program has been developed jointly by France, the European Commission, Belgium, Italy and Sweden. The instruments and associated ground services for data archival, processing and distribution have been operational since April 1998. Each 10-day synthesis was obtained through the compilation of the daily syntheses of ten consecutive days. They were computed using all passes acquired at each location during 10 day periods. The periods were defined as from the first to the tenth, from the 11th to the 20th, and from the 21st to the end of each month. Ten-day syntheses were generated with the 'best' measurement for the entire period, i.e., the maximum NDVI value. The 1 km spatial resolution was nearly constant across the whole 2,250 km swath covered, which meant that there was almost no distortion at the image edge (Maisongrande et al. 2004). The relationship between the digital number (DN) and the real NDVI can be calculated using the following formula: $\mathrm{NDVI} = a * \mathrm{DN} + b$, where coefficient a is 0.004 and coefficient b is -0.1.

In this research, a time series of 372 SPOT VEGETATION scenes, covering the period from 1998 to 2008, was obtained from the Environmental and Ecological Science Data Center for West China, National Natural Science Foundation of China (http://westdc.westgis.ac.cn).

The NDVI values of the 20 selected metrological stations were extracted from the SPOT VGT-S of China data according to the corresponding coordinate.

2.3 Methodology

Three analytical tools were used to evaluate the NDVI dynamic and its response to the regional climatic variables. Firstly, a wavelet transform was used to reveal the periodicity trend in changes and dynamic in the NDVI, including wavelet decomposition and reconstruction to approximate the NDVI in the study area over the entire study period at varying time scales. Secondly, the correlation between the NDVI and climatic variables was revealed by correlation analysis and the change cycle of the NDVI and climatic factors were extracted from the wavelet variance at the 20

selected stations. Lastly, quantitative relationship between the NDVI and the climate variables was revealed by regression analysis at the most suitable time scale.

2.3.1 Correlation analysis

The correlation is one of the most common and most useful statistical methods, which is a statistical measurement of the relationship between two variables (Zimmerman 1986). Possible correlations range from +1 to −1. A zero correlation indicates that there is no relationship between the variables. A negative correlation indicates that as one variable goes up, the other goes down. A positive correlation indicates that both variables move in the same direction together.

For the two variables, x and y, the correlation coefficient is calculated as:

$$r_{xy} = \frac{\sum_{i=1}^{n}(x_i - \bar{x})(y_i - \bar{y})}{\sqrt{\sum_{i=1}^{n}(x_i - \bar{x})^2}\sqrt{\sum_{i=1}^{n}(y_i - \bar{y})^2}} \quad (1)$$

where, n is the sample number; x_i represents the value of x for the sample i; y_i represents the value of y for the sample i; $\bar{x}$ is the mean for all x_i; $\bar{y}$ is the mean for all y_i. Commonly, testing the significance of the correlation coefficient employs the t distribution (Zimmerman 1986).

The correlation analysis was used to check the correlations between the NDVI and the related climate factors, such as temperature and precipitation in this study.

2.3.2 Wavelet analysis

Wavelet analysis is a recently developed method for signal and image processing. Analysis of time series using wavelet transform is a relatively new and powerful tool for describing processes that are multi-scale and non-stationary, occurring over finite spatial and temporal domains (Lau and Weng 1995). Wavelet transformation has been shown to be a powerful technique for characterization of the frequency, intensity, time position, and duration of variations in climate and hydrological time series (Xu et al. 2010, 2011a, b). Wavelet analysis can also reveal the localized time and frequency information without requiring the time series to be stationary, which required by the Fourier transform and other spectral methods.

A continuous wavelet function $\Psi(\eta)$ that depends on a non-dimensional time parameter η can be written as (Labat 2005):

$$\Psi(\eta) = \Psi(a,b) = |a|^{-1/2}\Psi\left(\frac{t-b}{a}\right) \quad (2)$$

where, t denotes time, a is the scale parameter and b is the translation parameter. $\Psi(\eta)$ must have a zero mean and be localized in both time and Fourier space (Farge 1992). The continuous wavelet transform (CWT) of a discrete signal, $x(t)$, such as the time series of NDVI, temperature or precipitation, is expressed by the convolution of $x(t)$ with a scaled and translated $\Psi(\eta)$,

$$W_x(a,b) = |a|^{-1/2}\int_{-\infty}^{+\infty} x(t)\Psi^*\left(\frac{t-b}{a}\right)dt \quad (3)$$

where, * indicates the complex conjugate, and $W_x(a, b)$ denotes the wavelet coefficient. Thus, the concept of frequency is replaced by that of scale, which can characterize the variation in the signal, $x(t)$ at a given time scale.

The wavelet variance that is used to detect the periods presents in the signal, $x(t)$ can be expressed as:

$$W_x(a) = \int_{-\infty}^{+\infty} |W_x(a,b)|^2 db \quad (4)$$

Selecting a proper wavelet function is a prerequisite for time series analysis. The actual criteria for wavelet selection including self-similarity, compactness and smoothness (Ramsey 1999). For the present study, Meyer wavelet was chosen as the base wavelet according to these criteria.

The nonlinear trend of a time series $x(t)$ can be analyzed at multiple scales through wavelet decomposition on the basis of the discrete wavelet transform (DWT). The DWT is defined taking discrete values of a and b. The full DWT for signal, $x(t)$, can be represented as (SG 1989):

$$x(t) = \sum_k \mu_{j_0,k}\phi_{j_0,k}(t) + \sum_{j=1}^{j_0}\sum_k \omega_{j,k}\psi_{j,k}(t) \quad (5)$$

where $\phi_{j_0,k}(t)$ and $\psi_{j,k}$ (t) are the flexing and parallel shift of the basic scaling function $\phi(t)$ the mother wavelet function $\psi(t)$, and $\mu_{j_0,k}(j<j_0)$ and $\omega_{j,k}$ are the scaling coefficients and the wavelet coefficients, respectively. Generally, scales and positions are based on powers of 2, which is the dyadic DWT.

Once a mother wavelet is selected, the wavelet transform can be used to decompose a signal according to scale, allowing separation of the fine-scale behavior (detail) from the large-scale behavior (approximation) of the signal (Bruce et al. 2002). The relationship between scale and signal behavior is designated as follows: low scale corresponds to compressed wavelet as well as rapidly changing details, named high frequency, whereas high scale corresponds to stretched wavelet and slowly changing coarse features, named low frequency. Signal decomposition is typically conducted in an iterative function using a series of scales such as a = 2, 4, 8, …, 2^n, with successive approximations being split in turn so that one signal is broken down into many lower resolution components.

2.3.3 Regression analysis

For understanding the response of NDVI to regional climate change, this paper also conducted a stepwise linear regression analysis to examine the response of the NDVI to climate change. The stepwise linear regression model involves automatic selection of independent variables. Stepwise regression can be achieved either by trying out one independent variable at a time and including it in the regression model if it is statistically significant, or by including all potential independent variables in the model and eliminating those that are not statistically significant, or by a combination of both methods. In our study, the dependent variable is NDVI and the independent variables are precipitation, temperature, relative humidity and sunshine hours. The multiple linear regression model is

$$Y = a_0 + a_1X_1 + a_2X_2 + \cdots + a_nX_n$$

where Y is dependent variable, a_i is the coefficient of the independent variables X_i. In this paper, the dependent variable is NDVI and the independent variables are climatic factors such as precipitation, temperature, relative humidity and sunshine hours.

3 Result and discussion

3.1 Dynamic of NDVI

NDVI dynamic gives us a whole understand about the NDVI distribution and changes during the study area. Different from the others studies, NDVI dynamic during the studied period were analyzed based on the remote sensing images using wavelet transform in this paper. Firstly, wavelet variance analysis was adapted to identity the NDVI change cycle during the study period. Secondly, the nonlinear change trend of NDVI was diagnosed based on wavelet transform and restructure, and then the mean NDVI and the time of the maximum NDVI were calculated based on the wavelet transform.

3.1.1 The vegetation cycle during the study period

Most plants begin growth at April and vanished at November, that is to say, plant has growth season and can reflect NDVI change cycle. For this reason, we analyzed the periodicity of the NDVI using data from 20 selected meteorological stations in the IM and computed the normalized wavelet variances as the method above. The normalized wavelet variance of the four selected stations shows in the Fig. 2 and the local maximal values list in the Table 2. From Fig. 2, we can clearly see that the wavelet variance at the four stations show similar pattern when they have the first local maximum value and the similar time scale at the first local maximum value, which indicates that they have the similar change cycle. Four selected stations, Tulihe, Arxan, Abag Banner and Urad Middle Banner, with forest, meadow steppe, typical steppe and desert steppe as their vegetation type, respectively, both show the change cycle with 29 ten-day in NDVI. We can see that there are no obvious differences in change cycles at different vegetation types. However, in the whole, the NDVI has the similar change cycle, about 290 days (29 ten-day), in different vegetation types. The nearly 290 days change cycle also implies that the vegetation growth cycle is nearly 10 months.

3.1.2 NDVI variation during the study period

Several mother wavelets can be found in literatures in the wavelet transform. The Sym8 orthogonal discrete wavelet

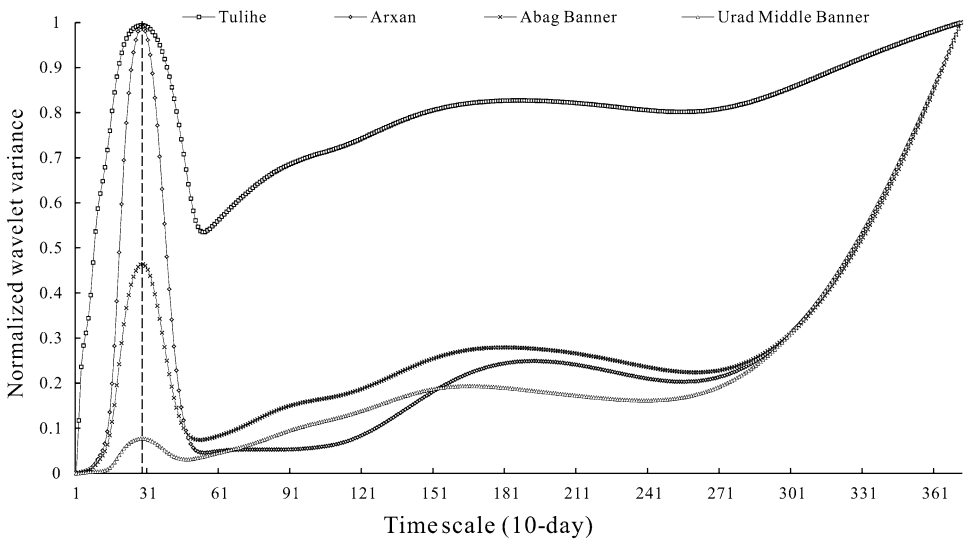

Fig. 2 Normalized wavelet variances of the NDVI at the four selected stations

Table 2 The maximum cycle (10 days) of NDVI, precipitation, temperature, relative humidity and sunshine hours at the 20 stations

	Site	NDVI	Precipitation	Temperature	Relative humidity	Sunshine hours	Vegetation types
1	Tulihe	29	29	29	183	29	Forest
2	Bugt	29	29	29	18	29	Forest
3	Hailar	28	29	29	34	28	Meadow steppe
4	Arxan	29	29	29	16	28	Meadow steppe
5	Duolun	29	29	29	35	30	Meadow steppe
6	Huade	29	29	29	35	29	Meadow steppe
7	Tongliao	28	29	29	30	28	Typical steppe
8	Jarud Banner	28	28	29	30	28	Typical steppe
9	Bairin Left Banner	29	28	29	30	29	Typical steppe
10	Chifeng	29	28	29	30	30	Typical steppe
11	Linxi	29	28	29	31	29	Typical steppe
12	West Ujimqin Banner	29	29	29	16	29	Typical steppe
13	Abag Banner	29	29	29	33	28	Typical steppe
14	Darhan United Banner	29	29	29	34	30	Typical steppe
15	Hohhot	28	29	29	33	29	Typical steppe
16	Erenhot	30	29	29	32	29	Desert steppe
17	Zhurihe	29	29	29	35	29	Desert steppe
18	Urad Middle Banner	29	29	29	32	29	Desert steppe
19	Jartai	28	28	28	32	30	Desert steppe
20	Bayan Mod	32	29	29	32	30	Desert steppe

has been chosen as the following reasons: (i) the existence of a scaling function for the numerical implementation of WT, (ii) its regularity condition that assures the smoothness of the reconstructed signal, (iii) the ease of implementation and, (iv) its low cost computation. The Sym8 wavelet has demonstrated successful results in land-cover changes analysis from time series of MODIS images (Freitas and Shimabukuro 2008) and multi-resolution analysis of global total ozone column from Nimbus-7 TOMS time series (Echer 2004).

In order to study the inter-annual and intra-annual components, the original NDVI time series was decomposed into five levels as mentioned above. Table 3 shows the period corresponding to the different scales for the Sym8 wavelet with a sampling period of 10 days (similar as in our NDVI time series).

Table 3 Scale and days corresponding to the different levels use Sym8 DWT

Level	Scale	Days
0	1	10
1	2	20
2	4	40
3	8	80
4	16	160
5	32	320

The process procedure was shown as Fig. 3. Firstly, original NDVI time series was built based on the different SPOT vegetation images at the Hailar station. From the original signal, cycled fluctuation was presented and some abrupt and abnormal values, in another word, noise were found. In order to remove the noise and make the overall trend and characters more clear, we decomposed and reconstructed the original signal, and extracted approximation part (represent A) and detail part (represent D) from it. The results are shown as Figs. 4, 5, 6, 7, and 8.

The wavelet decomposition for the time series of selected original NDVI signal at five time scales resulted in five variants of nonlinear trends (Figs. 4, 5, 6, 7, 8). At the time scale of 20-day (Fig. 4), the approximation part of S1 curve is smooth than the original but still retains a large amount of residual noise from the raw data (see Fig. 3 for a comparison). S1 curve shows 11 peaks while each peak has sub-peaks, and the corresponding detail part shows drastic fluctuations along the entire time span but the center is stable. These characteristics indicate that, although the NDVI varied greatly throughout the study period, there was a hidden relatively stable trend. At the time scale of 40-day (Fig. 5), the approximation part of S2 curve still retains a considerable amount of residual noise. However, it is much smoother than the S1 curve, which allows the hidden trend to be more apparent. At the time scale of 80-day (Fig. 6), the S3 curve retains much less residual noise, and presents obvious periodicity, as indicated by the 11 peaks and 10

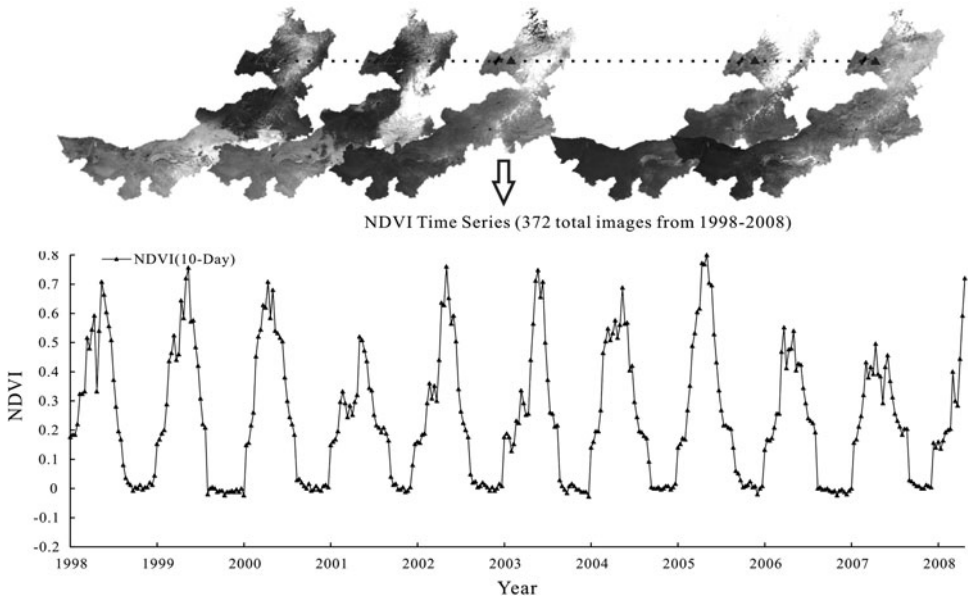

Fig. 3 NDVI time serials based on one pixel

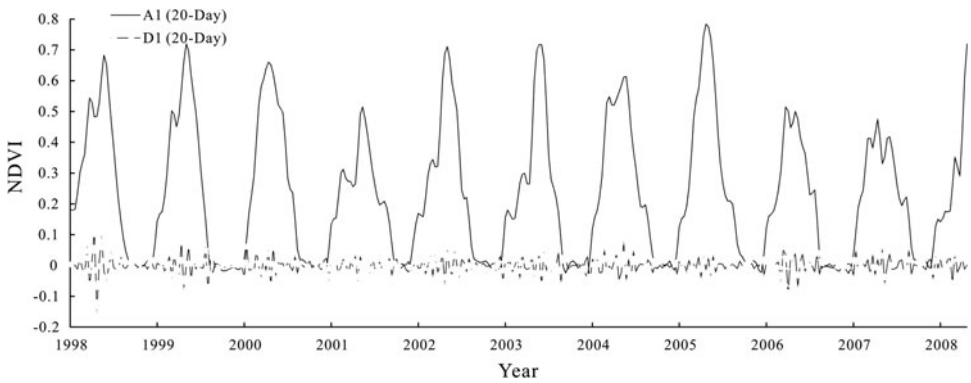

Fig. 4 NDVI series was decomposed and constructed at the S1 scale at the Hailar station

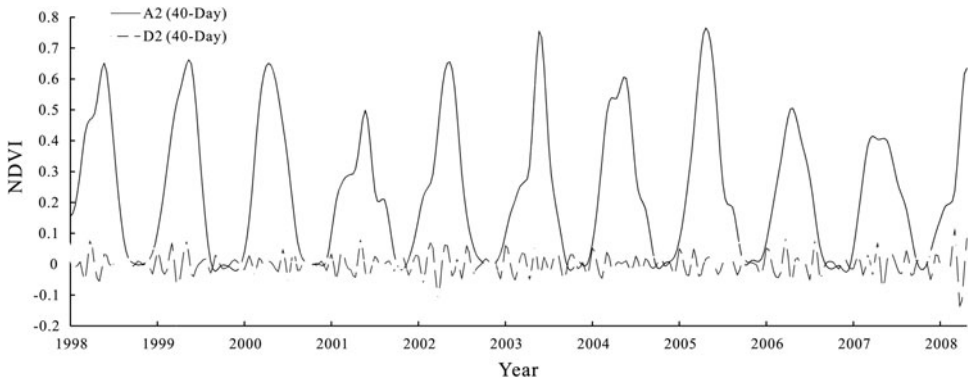

Fig. 5 NDVI series was decomposed and constructed at the S2 time scale at the Hailar station

valleys. Compared to S2, sub-peaks were eliminated and the stable trend in NDVI over time is more apparent in S3. Perceptibly, this trend is more obvious in the S4 curve at the time scale of 160-day (Fig. 7) than in the S3 curve. The S4 represents a nearly half-year cycle and the approximation and the detail part show the same cycle. Finally, the approximation part of S5 (Fig. 8) curve at the time scale of 320-day, a nearly 1 year cycle, presents a clear stable trend, and the detail part also clearly shows the abrupt change at the whole time series.

In order to link the vegetation dynamic with the wavelet construction component, three relevant outputs for our study are: (1) the variability component, $V = \sum_{j=1}^{5} Dj$, which refers to the sum of the detail components from level 1 up to level 5 and can be regarded as the total intra-annual variability, (2) the detail component D_4, which can be

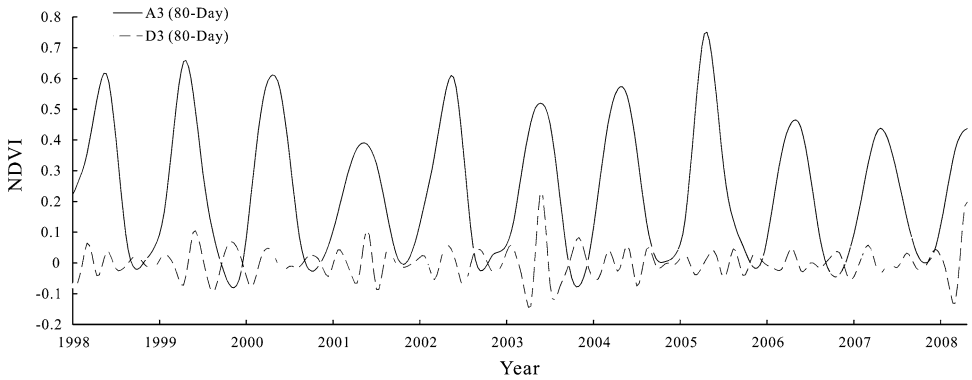

Fig. 6 NDVI series was decomposed and constructed at the S3 time scale at the Hailar station

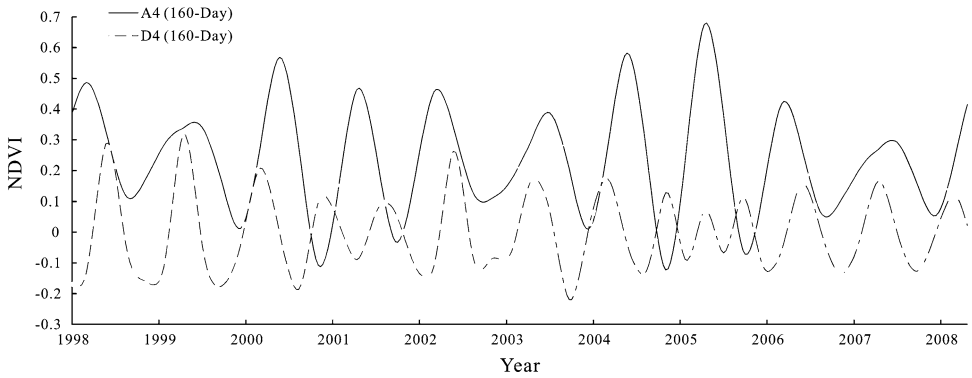

Fig. 7 NDVI series was decomposed and constructed at the S4 time scale at the Hailar station

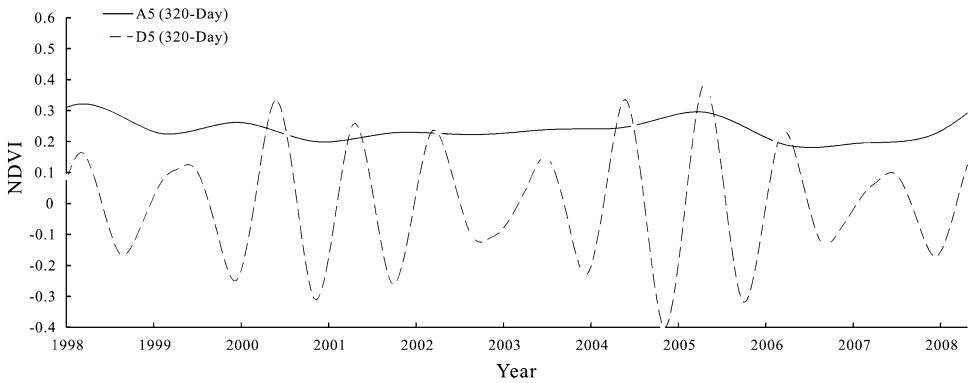

Fig. 8 NDVI series was decomposed and constructed at the S5 time scale at the Hailar station

related to semi-annual variations of seasonal cycle because its semi-period is 160 days, and (3) the component A_5, which describes inter-annual changes for its semi-period of 320 days. The methodology for studying vegetation dynamics using multi-resolution analysis (MRA) is divided into three steps. First, the MRA is applied to the NDVI image series to decompose the original series into the inter-annual A_5 and intra-annual V and D_5 series. The second step consists of different key features deriving from the above series, such as $\overline{NDVI}$, $\Delta NDVI$, and $T_{\max}$ (Table 4), which are related to vegetation phenology. All these parameters are potentially useful to study vegetation dynamics (Martínez and Gilabert 2009). $\overline{NDVI}$ is an indicator of the mean vegetation amount during the analyzed time range. $\Delta NDVI$ is the amplitude of the annual phenological cycle, without including noise due to the presence of outliers in the original signal. The timing of the maximum NDVI, $T_{\max}$, is considered as an important feature to characterize vegetation dynamics since it is related with the phenological cycle of each vegetation cover type. The third step contains the comprehensive identification of the NDVI changes with the trend of A_5.

According to step 2 of the methodology, a series of images can be calculated to study vegetation dynamics by applying the wavelet transform on the basis of per pixel. Figures 9, 10 and 11 show the images of $\overline{NDVI}$, $\Delta NDVI$ and $T_{\max}$, respectively. All have remarkable feature colors, and the features are easy to be identified.

The $\overline{NDVI}$ image (Fig. 9) shows compared information, with maximum values in the Great Khingan

Table 4 Key features computed by wavelet transform to study vegetation dynamics

Parameter	Description	Meaning
$\overline{NDVI}$	Mean of the inter-annual component $\overline{NDVI} = \overline{A_5}$	Mean NDVI level of vegetation during the period
$\Delta NDVI$	Range of percentiles 10 and 90% for the intra-annual variability: $\Delta NDVI = R10,90(V)$	Amplitude of the annual phenological cycle
T_{max}	Timing of the maximum NDVI corresponding to the D5 component	Date of maximum NDVI

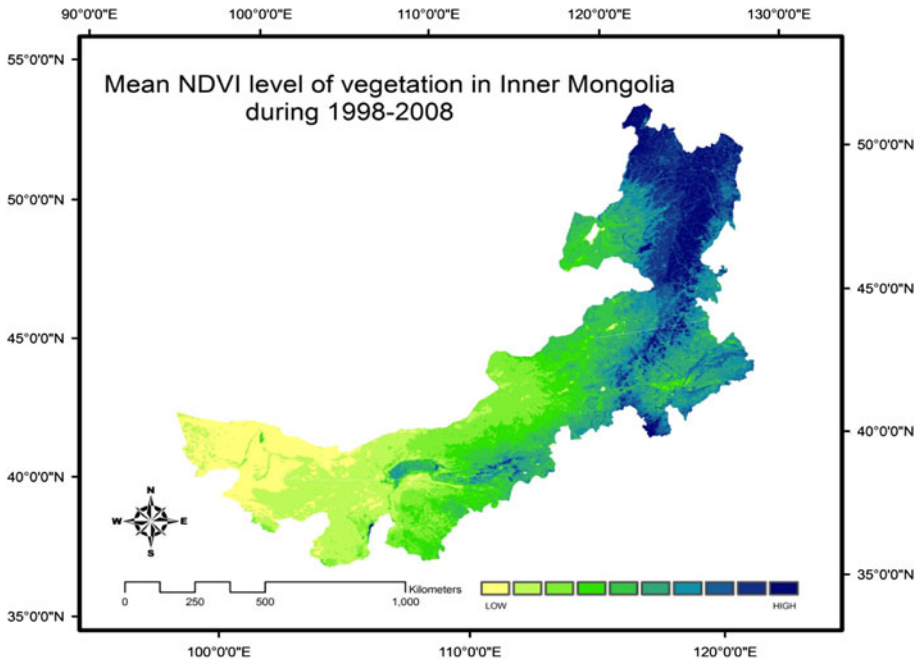

Fig. 9 Mean NDVI level of vegetation in Inner Mongolia during 1998–2008

Mountain Range and minimum values in the Badain Jaran Desert. The middle values are mainly located in the Nen Plain, Hetao Plain, Hulunbuir Grassland, Xilingol Grassland, and the Ulanqab Grassland. The NDVI distribution presents a trend that the values are decreased from northeast to southwest in the whole, but there exist high or low values at some special area such as Hetao Plain and Ordos Plateau due to the special geographic condition. The $\Delta NDVI$ image (Fig. 10) shows the similar pattern as $\overline{NDVI}$ image and it clearly identifies the Great Khingan Mountain Range and Badain Jaran Desert, which is corresponded to humid and dry regions, with the highest and lowest values, respectively.

Figure 11 shows the T_{max} image. Most pixels present values between August and October. Roughly speaking, vegetation peaking time is concentrated in August, September and October. August-peaking vegetation is mainly located in Great Khingan Mountain Range, Hetao Plain, and partial in Ordos Plateau and Nen Plain, where the vegetation type is forest in the Great Khingan Mountain Range and meadow steppe in the Nen Plain. Meantime, September-peaking vegetation mainly exists in Hulunbuir Grassland, Xilingol Grassland and Ulanqab Grassland, where the vegetation type is typical meadow. A special attention we should give is the west area of the Inner Mongolia, where exists large areas with dark blue color, indicating that the date of the maximum vegetation is October. Those areas are deserts and the vegetation cover is very low, then the NDVI reflects the rock or sand characters, so the T_{max} does not reflect the truth vegetation condition.

The distribution of the NDVI is affected by the combination of Asian monsoon and the special geographical location, affecting on the temperature and the precipitation distribution. Rainy season began in May because of the Asian monsoon, from then on, the vegetation started to grow, leading to an increase in the green area and a maximum NDVI value in August. Figure 9 shows that the vegetation cover was relatively high in the Great Khingan Mountain Range. It reflects the fact that the climate was warm and wet in these regions. On the other hand, the vegetation growth in the northwestern region was limited, resulting in a low NDVI value, which indicates that this region was very dry and the Asian monsoon influenced little. The time of the maximum NDVI value is coordinated with the result at the Tibet Plateau (Zhong et al. 2010).

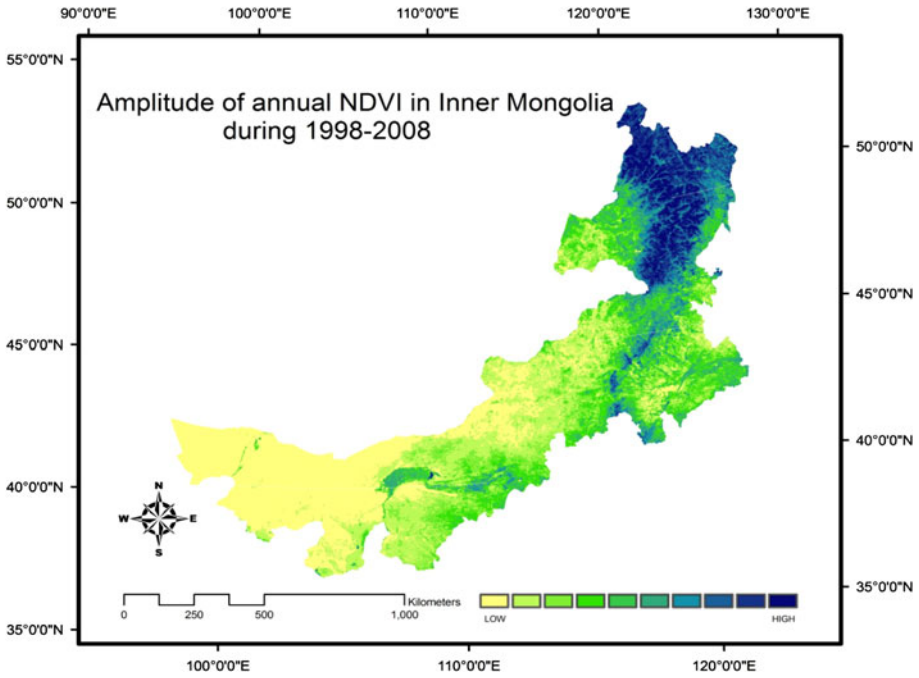

Fig. 10 Amplitude of annual NDVI in Inner Mongolia during 1998–2008

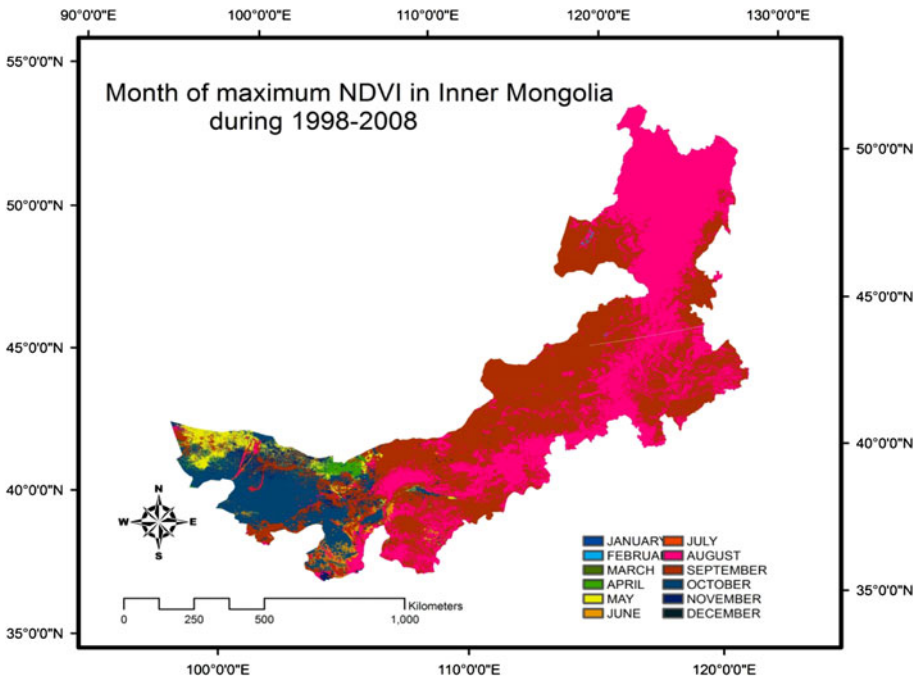

Fig. 11 Month of maximum NDVI in Inner Mongolia during 1998–2008

3.2 The response of vegetation dynamic to climate factors

3.2.1 The correlation between the NDVI and the relevant climatic factors

In order to investigate the relationships between NDVI and its climate factors in four typical vegetation types in the Inner Mongolia, the NDVI values nearest 20 meteorological stations listed in Table 1 was extracted from the SPOT Vegetation Images and then a correlation analysis was performed based on the times series of 372 data on NDVI, precipitation (P), temperature (T), relative humidity (H) and sunshine hours (S). The result shows as Table 5.

Different vegetation cover types showed different strengths in correlation between NDVI and climate variables, but the correlation values between NDVI and precipitation and temperature decreased from meadow steppe

Table 5 The correlation coefficients between NDVI and climatic factors

No.	Station	NDVI vs P	NDVI vs T	NDVI vs H	NDVI vs S	Vegetation types
1	Tulihe	0.606**	0.864**	0.277**	0.375**	Forest
2	Bugt	0.499**	0.876**	0.253**	0.363**	Forest
3	Hailar	0.489**	0.857**	−0.323**	0.548**	Meadow steppe
4	Arxan	0.575**	0.874**	0.071	0.422**	Meadow steppe
5	Duolun	0.539**	0.846**	0.195**	0.222**	Meadow steppe
6	Huade	0.493**	0.726**	0.115*	0.308**	Meadow steppe
7	Tongliao	0.428**	0.754**	0.549**	0.189**	Typical steppe
8	Jarud Banner	0.340**	0.694**	0.568**	0.097	Typical steppe
9	Bairin Left Banner	0.328**	0.634**	0.574**	0.365**	Typical steppe
10	Chifeng	0.462**	0.712**	0.620**	0.352**	Typical steppe
11	Linxi	0.481**	0.788**	0.531**	0.390**	Typical steppe
12	West Ujimqin Banner	0.473**	0.851**	−0.110*	0.519**	Typical steppe
13	Abag Banner	0.436**	0.789**	−0.341**	0.501**	Typical steppe
14	Darhan United Banner	0.480**	0.754**	−0.048	0.316**	Typical steppe
15	Hohhot	0.515**	0.721**	0.228**	0.381**	Typical steppe
16	Erenhot	0.297**	0.600**	−0.349**	0.369**	Desert steppe
17	Zhurihe	0.456**	0.696**	−0.075	0.414**	Desert steppe
18	Urad Middle Banner	0.340**	0.721**	−0.234**	0.505**	Desert steppe
19	Jartai	0.154**	0.573**	−0.182**	0.371**	Desert steppe
20	Bayan Mod	0.157**	0.415**	−0.179**	0.267**	Desert steppe

Note:** Correlation is significant at the 0.01 level (2-tailed) * Correlation is significant at the 0.05 level (2-tailed)

to desert steppe in the whole. The relation between NDVI and temperature is most closed, followed by precipitation, sunshine hours and relative humidity. NDVI has a positive correlation with precipitation, temperature and sunshine hours but a negative correlation with relative humidity at some sites. In meadow steppe (Hailar and Arxan station) at the north part of Inner Mongolia, the maximum NDVI is relatively high, with 0.8 and 0.848 (Table 6) and the mean NDVI is 0.236 and 0.292 (Table 7) in this two sites, respectively. The minimum NDVI is less than zero. The reason for this phenomenon is that in winter the two sites may be covered by snow and the NDVI of the snow or ice is less than zero. The precipitation in the two sites is abundant while the temperature is low (−1.5 and 0.5°C). So the temperature is the limited factor in this area and has a more closed relationship with the NDVI. In the southern Inner Mongolia meadow steppe (Duolun and Huade station), the maximum and mean NDVI is smaller than the north part, and the reason for this is that the precipitation is a little smaller than northern meadow steppe (Table 6) on the effect of local geographic environment. But in the whole, the correlation between NDVI and precipitation and temperature are more closed in meadow steppe than other types. In desert steppe, the maximum NDVI is low, with the range from 0.136 to 0.316 (Table 6) and the mean NDVI from 0.079 to 0.140 but the temperature is relatively high (from 5.8 to 10.2°C). The small amount of precipitation (33.09 mm) greatly limited vegetation growth during a whole year (Table 7). The high temperature there (annual mean temperature), was another limited factor for high evaporation. Therefore, the correlation is weak and the vegetation hardly grow, even in the growing season. For the typical steppe, the correlations between NDVI and climate parameters are at the middle level and the temperature and precipitation has a complex limitation on the vegetation growth. Our results has not supported previous analysis, which suggested that the precipitation and the temperature were the two main factors in vegetation growth and NDVI was more related with the precipitation than temperature in the arid and semi-arid area. In our study, the NDVI was more related with the temperature than precipitation, and temperature, sunshine hours and precipitation are the three main factors.

3.2.2 The similar periodicity between NDVI and the climatic factors

From the previous analysis, we know that there are obvious correlations between NDVI and the climatic factors. It indicates that the climate change can impact the change of NDVI in the IM. So, it is necessary to determine whether there is a similar cycle pattern with NDVI in the related variables. For this reason, we analyze the periodicity of climatic factors to reveal its relationship.

Table 6 The maximum, minimum and average NDVI values for different vegetation types

No.	Station	Maximum	Minimum	Average	SD	Vegetation types
1	Tulihe	0.888	−0.004	0.317	0.287	Forest
2	Bugt	0.888	−0.024	0.364	0.296	Forest
3	Hailar	0.800	−0.028	0.236	0.221	Meadow steppe
4	Arxan	0.848	−0.024	0.292	0.272	Meadow steppe
5	Duolun	0.620	0.012	0.243	0.133	Meadow steppe
6	Huade	0.612	0.004	0.206	0.120	Meadow steppe
7	Tongliao	0.656	0.02	0.269	0.148	Typical steppe
8	Jarud Banner	0.664	0.004	0.246	0.131	Typical steppe
9	Bairin Left Banner	0.660	0.016	0.253	0.140	Typical steppe
10	Chifeng	0.752	0.024	0.265	0.159	Typical steppe
11	Linxi	0.716	0	0.291	0.162	Typical steppe
12	West Ujimqin Banner	0.652	−0.012	0.230	0.180	Typical steppe
13	Abag Banner	0.476	−0.012	0.156	0.103	Typical steppe
14	Darhan United Banner	0.412	−0.008	0.163	0.076	Typical steppe
15	Hohhot	0.644	0.004	0.223	0.147	Typical steppe
16	Erenhot	0.264	−0.004	0.115	0.041	Desert steppe
17	Zhurihe	0.316	−0.008	0.140	0.063	Desert steppe
18	Urad Middle Banner	0.224	0.000	0.112	0.034	Desert steppe
19	Jartai	0.136	−0.004	0.089	0.019	Desert steppe
20	Bayan Mod	0.164	−0.008	0.079	0.020	Desert steppe

Table 7 Mean NDVI, precipitation, temperature, sunshine hours and relative humidity values for different vegetation types

No.	Station	Mean NDVI	Mean P (0.1 mm)	Mean T (0.1°C)	Mean H (1%)	Mean S (h)	Vegetation types
1	Tulihe	0.317	105.29	−34.33	68.84	711.21	Forest
2	Bugt	0.364	119.81	5.17	62.72	780.74	Forest
3	Hailar	0.236	93.74	5.31	64.27	668.20	Meadow steppe
4	Arxan	0.292	110.41	−15.36	66.96	790.37	Meadow steppe
5	Duolun	0.243	106.86	36.66	58.90	780.45	Meadow steppe
6	Huade	0.206	88.96	41.20	57.00	797.16	Meadow steppe
7	Tongliao	0.269	94.27	79.29	53.35	829.11	Typical steppe
8	Jarud Banner	0.246	92.76	79.21	46.70	808.72	Typical steppe
9	Bairin Left Banner	0.253	99.09	68.45	49.73	876.13	Typical steppe
10	Chifeng	0.265	95.14	82.72	49.5	799.84	Typical steppe
11	Linxi	0.291	96.12	59.67	48.74	814.6	Typical steppe
12	West Ujimqin Banner	0.230	81.85	29.90	57.42	772.15	Typical steppe
13	Abag Banner	0.156	65.27	31.07	53.12	817.40	Typical steppe
14	Darhan United Banner	0.163	74.05	56.21	47.69	824.8	Typical steppe
15	Hohhot	0.223	110.54	84.07	49.6	750.59	Typical steppe
16	Erenhot	0.115	33.09	58.27	45.42	866.65	Desert steppe
17	Zhurihe	0.140	54.97	64.25	45.38	871.79	Desert steppe
18	Urad Middle Banner	0.112	54.78	67.74	47.57	858.62	Desert steppe
19	Jartai	0.089	30.52	102.54	39.48	925.37	Desert steppe
20	Bayan Mod	0.079	33.46	84.22	39.33	922.6	Desert steppe

Using the data on precipitation, temperature, relative humidity and sunshine hours from 20 selected meteorological stations in the IM, we computed the normalized wavelet variances as the method above, and then computed the local maximal values, listed in Table 2. Figure 12 shows the normalized wavelet variances in the Hailar

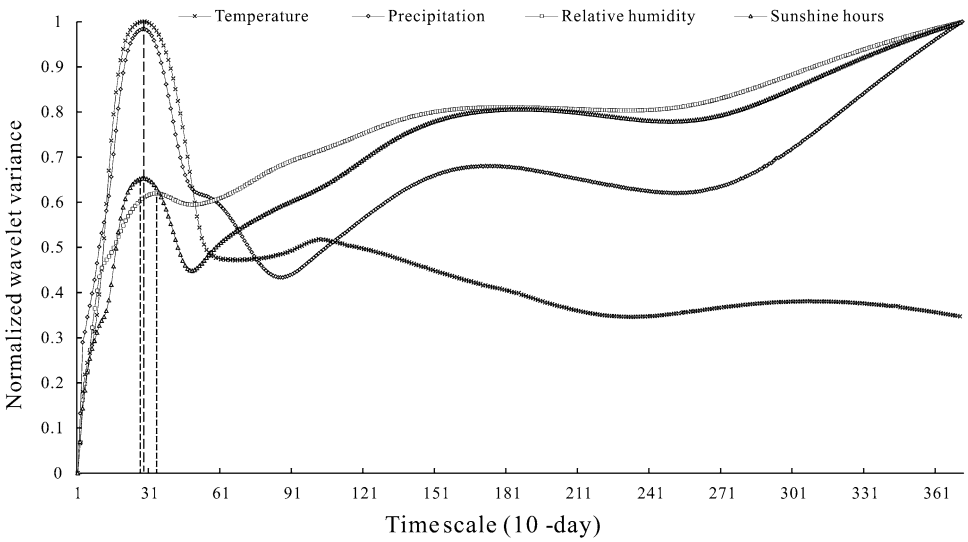

Fig. 12 The normalized wavelet variance of the climate factors in the Hailar station

station, and the other stations' figures are not shown, because the method and the figure are similar. Figure 12 tells us that the series for the precipitation, temperature, relative humidity and sunshine hours locally maximized in the 29, 29, 34 and 28 10-days, respectively. The results imply that there were 290, 290, 340 and 280 days cycle for precipitation, temperature, relative humidity and sunshine hours in the Hailar station over the study period of 1998–2008, respectively, which is approximately corresponds to the 280 days cycle for the NDVI (see NDVI in Table 2 as reference). In other words, the precipitation and temperature present a same periodicity, i.e., 290 days cycle, and the NDVI has a similar 280 days cycle.

From the Table 2, we can see that the precipitation, the temperature and the sunshine hours have the similar 280 or 290 change cycle in the 20 selected stations. The ten stations, i.e.Tulihe, Bugt, Arxan, Duolun, Huade, West Ujimqin Banner, Abag Banner, Darhan United Banner, Zhurihe and Urad Middle Banner, show the same change cycle with 290 days among NDVI, precipitation and temperature, while the rest ten stations show nearly 290 days change cycle in NDVI, which is 10 days earlier or later than precipitation and temperature. We can see that there are no obvious differences in change cycles at different vegetation types. However, in the whole, we can see that the NDVI has the similar change cycle with the temperature, precipitation and sunshine hours, which supports the close correlation between NDVI and its climatic factors from a new perspective.

3.2.3 The quantitative relation between NDVI and its related climatic factors

The similar periodicity between NDVI and the climatic factors indicates that there may be a correlation between the NDVI and its relevant climatic factors. In order to figure out the suitable time scale to interpret the vegetation dynamic responses to climatic factors and establish quantitative relation between them. Taking Hailar station as example, we fitted the regression equations for describing the correlations between NDVI and its related climatic factors at different scales firstly and then found out the most suitable regression equations to identity the best time scale based on the results of wavelet decomposition and reconstruction on NDVI and climatic factors at different time scales. It's showed in Table 8 that, from S0 (10 days) to S5 (320 days), the vegetation dynamic is more closed with temperature at a short time scale and as time scale increased, the precipitation plays an increased important role in vegetation dynamic. All regression equations at S0, S1, S2, S3, S4, and S5 (i.e., at the time scale of 10, 20, 40, 80, 160, and 320-day) are significant, which indicates that the vegetation dynamic is significantly correlated to the temperature and precipitation at the time scale of 10, 20, 40, 80, 160, and 320-day, respectively. Among the six time scales, the regression at S3 (i.e., the time scale of 80-day) is most significant, and this indicates that the 80-day, nearly three months (one season) scale is most suitable for evaluating the vegetation dynamic to climatic factors.

As the methods above, the regression equations between NDVI and climatic factors at nine selected stations (Tulihe, Bugt, Hailar, Arxan, West Ujimqin Banner, Abag Banner, Erenhot, Urad Middle Banner and Jartai) at six time scales was fitted and then the most suitable time scale was selected and listed in Table 9. Table 9 shows that the most suitable scale was S3 (80-day) excepting the Erenhot station with S5 (320-day) at the nine selected stations. So the 80-day, nearly 3 months (one season) scale is most suitable for evaluating the vegetation dynamic to climatic factors.

Table 8 The regression equation between NDVI and climatic factors at different time scales in Hailar station

Time scale	Regression equation	R^2	F	Significance level α
S0	N = 0.00107*T + 0.00017*P + 0.2148	0.744	537	0.001
S1	N = 0.00318*T + 0.00001*P + 0.2010	0.770	616	0.001
S2	N = 0.00091*T + 0.00056*P + 0.179	0.807	771	0.001
S3	N = 0.00082*T + 0.00079*P + 0.158	0.854	1079	0.001
S4	N = 0.00037*T + 0.00148*P + 0.095	0.520	200	0.001
S5	N = 0.00027*T + 0.00118*P + 0.128	0.509	190	0.001

Note: *N* 10-day maximum NDVI, *P* 10-day average precipitation, *T* 10-day annual temperature

Table 9 The regression equation between NDVI and climatic factors at most suitable time scales in nine selected stations

Site	Regression equation	R_2	F	Significance level α	Most suitable scale
Tulihe	N = 0.00107*T + 0.00093*P + 0.2558	0.843	988	0.001	S3
Bugt	N = 0.00167*T + 0.00026*P + 0.3245	0.851	1051	0.001	S3
Hailar	N = 0.00082*T + 0.00079*P + 0.158	0.854	1079	0.001	S3
Arxan	N = 0.00113*T + 0.00081*P + 0.2195	0.861	1144	0.001	S3
West Ujimqin Banner	N = 0.00076*T + 0.00066*P + 0.1534	0.839	964	0.001	S3
Abag Banner	N = 0.00039*T + 0.00038*P + 0.1200	0.728	494	0.001	S3
Erenhot	N = 0.00016*T +0.00080*P + 0.0794	0.559	234	0.001	S5
Urad Middle Banner	N = 0.00016*T + 0.00007*P + 0.0978	0.652	345	0.001	S3
Jartai	N = 0.00007*T + 0.00007*P + 0.0804	0.442	145	0.001	S3

Note: *N* 10-day maximum NDVI, *P* 10-day average precipitation, *T* 10-day annual temperature

4 Conclusions

In this study, we diagnosed the NDVI dynamic in the Inner Mongolia using the 9-year period of SPOT NDVI images based on wavelet transform. Spatial and temporal vegetation changes were investigated. The NDVI data and the corresponding climatic data on precipitation and temperature were analyzed using correlation analysis method. And the change cycle of the vegetation and its climatic factors were investigated and then the quantitative relationship between them was given at the different time scales.

From the previous analysis and results we concluded:

1. Wavelet transform is an effective tool for removing noise and abrupt data from vegetation time series, and the indices abstracted from the wavelet transform can well describe the vegetation spatial and temporal distribution in the whole area. From the analysis, we get the results that the overall distribution presents trends that the NDVI decreased from northeast to southwest in the whole, but high or low values at some special area such as Hetao Plain and Ordos Plateau due to the special geographic condition. And vegetation peaking time is concentrated in August, September and October. This phenomenon was affected by the Asia monsoon and the local geographical environment.
2. There are strong correlations between NDVI and precipitation, temperature, relative humidity and sunshine hours, respectively. The relation between NDVI and temperature is most close, followed by sunshine hours, precipitation and relative humidity. NDVI have a positive correlation between precipitation, temperature and sunshine hours but a negative correlation between relative humidity. Different vegetation cover types showed different strengths in correlation between NDVI and climate variables and the correlation values decreased from meadow steppe to desert steppe in the whole.
3. The precipitation and the temperature have the same change cycle, with nearly 290 days change cycle, in the 20 selected stations. The NDVI has the similar change cycle with the precipitation and temperature or either 10 days earlier or later than precipitation and temperature, supporting the close correlation between NDVI and its climatic factors in a new perspective. There are no obvious differences in change cycles at different vegetation types. The nearly 290 days change

cycle implies that the vegetation growth cycle is nearly 10 months.

4. The quantitative relation between NDVI and its related climatic factors at the nine selected stations were given by regression analysis at most suitable scale among the six scales, and S3 scale (80-day), nearly 3 months (one season), is most suitable for evaluating the vegetation dynamic to climatic factors.

Acknowledgments This work was supported by National Natural Science Foundation of China (Grant No. 41040015), and the Open Project of the Key Lab of Oasis Ecology of the Education Ministry PRC, Xinjiang University (Grant No. xjdx0201-2006001).

References

Asrar G, Fuchs M, Kanemasu E, Hatfield J (1984) Estimating absorbed photosynthetic radiation and leaf area index from spectral reflectance in wheat. Agron J 76:300–306

Azzali S, Menenti M (2000) Mapping vegetation-soil-climate complexes in southern Africa using temporal Fourier analysis of NOAA-AVHRR NDVI data. Int J Remote Sens 21(5):973–996

Borak JS, Lambin EF, Strahler AH (2000) The use of temporal metrics for land cover change detection at coarse spatial scales. Int J Remote Sens 21(6):1415–1432

Bradley BA, Jacob RW, Hermance JF, Mustard JF (2007) A curve fitting procedure to derive inter-annual phenologies from time series of noisy satellite NDVI data. Remote Sens Environ 106(2): 137–145

Bruce LM, Koger CH, Jiang L (2002) Dimensionality reduction of hyperspectral data using discrete wavelet transform feature extraction. Geosci Remote Sens IEEE Trans 40(10):2331–2338

Bruzzone L, Smits PC, Tilton JC (2003) Foreword special issue on analysis of multitemporal remote sensing images. Geosci Remote Sens IEEE Trans 41(11):2419–2422

Cao M, Woodward FI (1998) Dynamic responses of terrestrial ecosystem carbon cycling to global climate change. Nature 393(6682):249–252

Chamaille-Jammes S, Fritz H, Murindagomo F (2006) Spatial patterns of the NDVI-rainfall relationship at the seasonal and interannual time scales in an African savanna. Int J Remote Sens 27(23):5185–5200

Churkina G, Running SW (1998) Contrasting climatic controls on the estimated productivity of global terrestrial biomes. Ecosystems 1(2):206–215

Coppin P, Jonckheere I, Nackaerts K, Muys B, Lambin E (2004) Review ArticleDigital change detection methods in ecosystem monitoring: a review. Int J Remote Sens 25(9):1565–1596

Davenport ML, Nicholson SE (1993) On the relation between rainfall and the Normalized Difference Vegetation Index for diverse vegetation types in East Africa. Int J Remote Sens 14(12): 2369–2389

de Beurs KM, Henebry GM (2005) A statistical framework for the analysis of long image time series. Int J Remote Sens 26(8): 1551–1573

Diodato N, Bellocchi G (2008) Modelling vegetation greenness responses to climate variability in a Mediterranean terrestrial ecosystem. Environ Monit Assess 143(1–3):147–159. doi:10.1007/s10661-007-9964-z

Echer E (2004) Multi-resolution analysis of global total ozone column during 1979?1992 Nimbus-7 TOMS period. Ann Geophys 22(5): 1487–1493

Eidenshink JC, Faundeen JL (1994) The 1 km AVHRR global land data set: first stages in implementation. Int J Remote Sens 15(17): 3443–3462

Fabricante I, Oesterheld M, Paruelo JM (2009) Annual and seasonal variation of NDVI explained by current and previous precipitation across Northern Patagonia. J Arid Environ 73(8):745–753

Farge M (1992) Wavelet transforms and their applications to turbulence. Annu Rev Fluid Mech 24:395–457. doi:10.1146/annurev.fl.24.010192.002143

Freitas RM, Shimabukuro YE (2008) Combining wavelets and linear spectral mixture model for MODIS satellite sensor time-series analysis. J Comput Interdiscip Sci 1(1):51–56

Galford GL, Mustard JF, Melillo J, Gendrin A, Cerri CC, Cerri CEP (2008) Wavelet analysis of MODIS time series to detect expansion and intensification of row-crop agriculture in Brazil. Remote Sens Environ 112(2):576–587

Goward SN, Dye DG (1987) Evaluating North American net primary productivity with satellite observations. Adv Space Res 7(11): 165–174

Hall-Beyer M (2003) Comparison of single-year and multiyear NDVI time series principal components in cold temperate biomes. Geosci Remote Sens IEEE Trans 41(11):2568–2574

Hirosawa Y, Marsh SE, Kliman DH (1996) Application of standardized principal component analysis to land-cover characterization using multitemporal AVHRR data. Remote Sens Environ 58(3): 267–281

Jobbágy EG, Sala OE, Paruelo JM (2002) Patterns and controls of primary production in the Patagonian steppe: a remote sensing approach. Ecology 83(2):307–319

Jönsson P, Eklundh L (2004) TIMESAT-a program for analyzing time-series of satellite sensor data. Comput Geosci 30(8): 833–845

Kaufmann RK, Zhou L, Myneni RB, Tucker CJ, Slayback D, Shabanov NV, Pinzon J (2003) The effect of vegetation on surface temperature: a statistical analysis of NDVI and climate data. Geophys Res Lett 30(22):2147. doi:10.1029/2003GL018251

Knapp AK, Smith MD (2001) Variation among biomes in temporal dynamics of aboveground primary production. Science 291(5503): 481–484. doi:10.1126/science.291.5503.481

Labat D (2005) Recent advances in wavelet analyses: part 1. A review of concepts. J Hydrol 314(1–4):275–288

Lau KM, Weng H (1995) Climate signal detection using wavelet transform: how to make a time series sing. Bull Am Meteorol Soc 76(12):2391–2402

Maisongrande P, Duchemin B, Dedieu G (2004) VEGETATION/SPOT: an operational mission for the Earth monitoring; presentation of new standard products. Int J Remote Sens 25(1):9–14

Mallat SG (1989) A theory for multiresolution signal decomposition: the wavelet representation. IEEE Trans Pattern Anal Mach Intell 11(7):674–693

Malo A, Nicholson S (1990) A study of rainfall and vegetation dynamics in the African Sahel using normalized difference vegetation index. J Arid Environ 19:1–24

Martínez B, Gilabert MA (2009) Vegetation dynamics from NDVI time series analysis using the wavelet transform. Remote Sens Environ 113(9):1823–1842

Nemani RR, Keeling CD, Hashimoto H, Jolly WM, Piper SC, Tucker CJ, Myneni RB, Running SW (2003) Climate-driven increases in global terrestrial net primary production from 1982 to 1999. Science 300(5625):1560–1563

Nicholson SE, Farrar TJ (1994) The influence of soil type on the relationships between NDVI, rainfall, and soil moisture in

semiarid Botswana. I. NDVI response to rainfall. Remote Sens Environ 50(2):107–120

Pielke RA, Avissar R, Raupach M, Dolman AJ, Zeng XB, Denning AS (1998) Interactions between the atmosphere and terrestrial ecosystems: influence on weather and climate. Glob Change Biol 4(5):461–475

Prince SD (1991) Satellite remote sensing of primary production: comparison of results for Sahelian grasslands 1981–1988. Int J Remote Sens 12(6):1301–1311

Ramsey JB (1999) Regression over timescale decompositions: a sampling analysis of distributional properties. Econ Syst Res 11(2):163–184

Sakamoto T, Yokozawa M, Toritani H, Shibayama M, Ishitsuka N, Ohno H (2005) A crop phenology detection method using time-series MODIS data. Remote Sens Environ 96(3–4):366–374

Schultz PA, Halpert MS (1993) Global correlation of temperature, NDVI and precipitation. Adv Space Res 13(5):277–280

Stockli R, Vidale PL (2004) European plant phenology and climate as seen in a 20-year AVHRR land-surface parameter dataset. Int J Remote Sens 25(17):3303–3330. doi:10.1080/01431160310001618149

Tucker CJ, Vanpraet CL, Sharman MJ, Van Ittersum G (1985) Satellite remote sensing of total herbaceous biomass production in the Senegalese Sahel: 1980–1984. Remote Sens Environ 17(3):233–249

Udelhoven T, Stellmes M, del Barrio G, Hill J (2009) Assessment of rainfall and NDVI anomalies in Spain (1989–1999) using distributed lag models. Int J Remote Sens 30(8):1961–1976

Wang J, Rich PM, Price KP (2003) Temporal responses of NDVI to precipitation and temperature in the central Great Plains, USA. Int J Remote Sens 24(11):2345–2364

Wang H, Li X, Long H, Zhu W (2009) A study of the seasonal dynamics of grassland growth rates in Inner Mongolia based on AVHRR data and a light-use efficiency model. Int J Remote Sens 30(14):3799–3815

Xu JH, Li WH, Ji MH, Lu F, Dong S (2010) A comprehensive approach to characterization of the nonlinearity of runoff in the headwaters of the Tarim River, Western China. Hydrol Process 24(2):136–146. doi:10.1002/hyp.7484

Xu JH, Chen YN, Li WH, Yang Y, Hong YL (2011a) An integrated statistical approach to identify the nonlinear trend of runoff in the Hotan River and its relation with climatic factors. Stoch Environ Res Risk Assess 25(2):223–233. doi:10.1007/s00477-010-0433-9

Xu JH, Chen YN, Lu F, Li WH, Zhang LJ, Hong YL (2011b) The nonlinear trend of runoff and its response to climate change in the Aksu River, western China. Int J Climatol 31(5):687–695. doi:10.1002/joc.2110

Zeng B, Yang TB (2008) Impacts of climate warming on vegetation in Qaidam Area from 1990 to 2003. Environ Monit Assess 144(1–3):403–417. doi:10.1007/s10661-007-0003-x

Zhong L, Ma Y, Salama M, Su Z (2010) Assessment of vegetation dynamics and their response to variations in precipitation and temperature in the Tibetan plateau. Clim Chang 1–17. doi:10.1007/s10584-009-9787-8

Zimmerman DW (1986) Tests of significance of correlation coefficients in the absence of bivariate normal populations. J Exp Educ 54(4):223–227